EVOLUTION OF CHANGES IN MEAN-SQUARE CHARGE RADII IN CALIFORNIUM ISOTOPES

Kenneth van Beek

For the RADRIS collaboration

Technische Universität Darmstadt, Germany

GSI Helmholtzzentrum für Schwerionenforschung GmbH, Darmstadt, Germany

HEAVY ELEMENTS: FAR FROM STABILITY

TECHNISCHE UNIVERSITÄT DARMSTADT

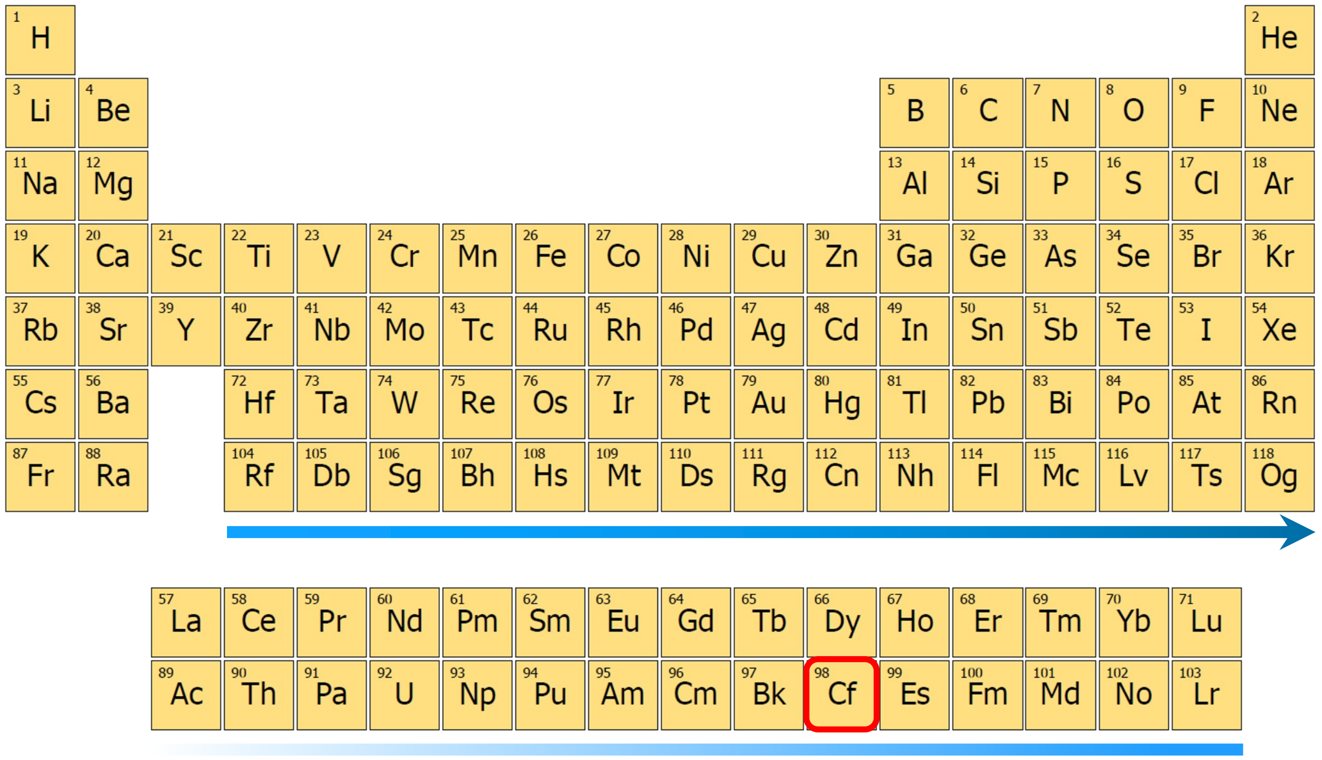

Macroscopic instability

Fission barrier diminishes
$$B_{\mathrm{f}} \rightarrow 0$$

Microscopic stabilization

Shell effects

Pairing

(Super) heavy elements owe their existence to shell effects

Studying their properties provide stringest tests of nuclear models

PHYSICS OF HEAVY ELEMENTS

TECHNISCHE UNIVERSITÄT DARMSTADT

Nuclear Structure

Quadrupole Deformation

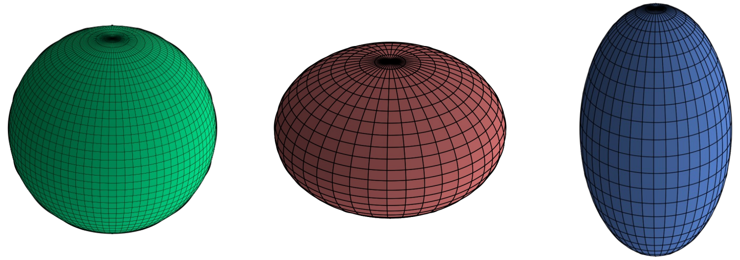

$Q_S = 0$	$Q_S < 0$	$Q_S > 0$
Spherical	Oblate	Prolate

- Rare in heavier systems
- Normally found around magic N, Z

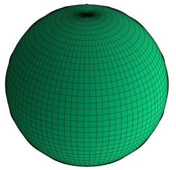

- Prevalent deformation (in heavy actinides)
- Often minimizes the nucleus' total energy

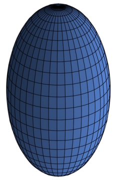

- Oblate g.s. more common in lighter nuclei
- Often coexists with prolate deformation

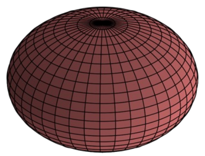

- Exotic triaxiality (no symmetry axis) can occur

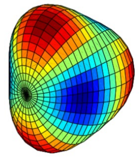

- Higher order multipoles (pear shaped Ra-224)

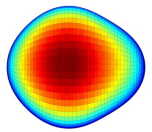

PHYSICS OF HEAVY ELEMENTS

TECHNISCHE UNIVERSITÄT DARMSTADT

Isotope Shift

Frequency shift of an electronic transition for different N

$$\boxed{\delta\nu^{A,A'}} = \boxed{\frac{m^{A'} - m^{A}}{m^{A'} \cdot m^{A}}} \cdot \boxed{\mathrm{K}} + \boxed{\mathrm{F}} \boxed{\delta\langle r^2\rangle^{A,A'}}$$

Property connects electronic shell with nucleus

Not to be confused with the (inverse) of the reduced mass

$$F = F\left(\langle r^2\rangle, \langle r^4\rangle, \langle r^6\rangle, \ldots\right)$$

$$V(r=0) \neq \infty$$

$$m_{\text{Nucl.}} \neq \infty$$

COM motion

Field Shift F

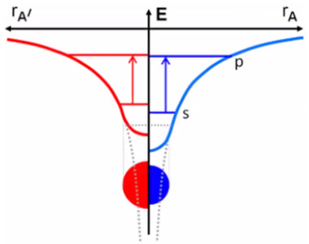

Dominant contribution in heavy systems

Mass Shift K

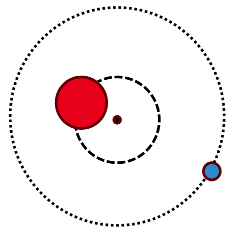

NMS

+

SMS

DERIVING NUCLEAR PROPERTIES FROM LASER SPECTROSCOPY

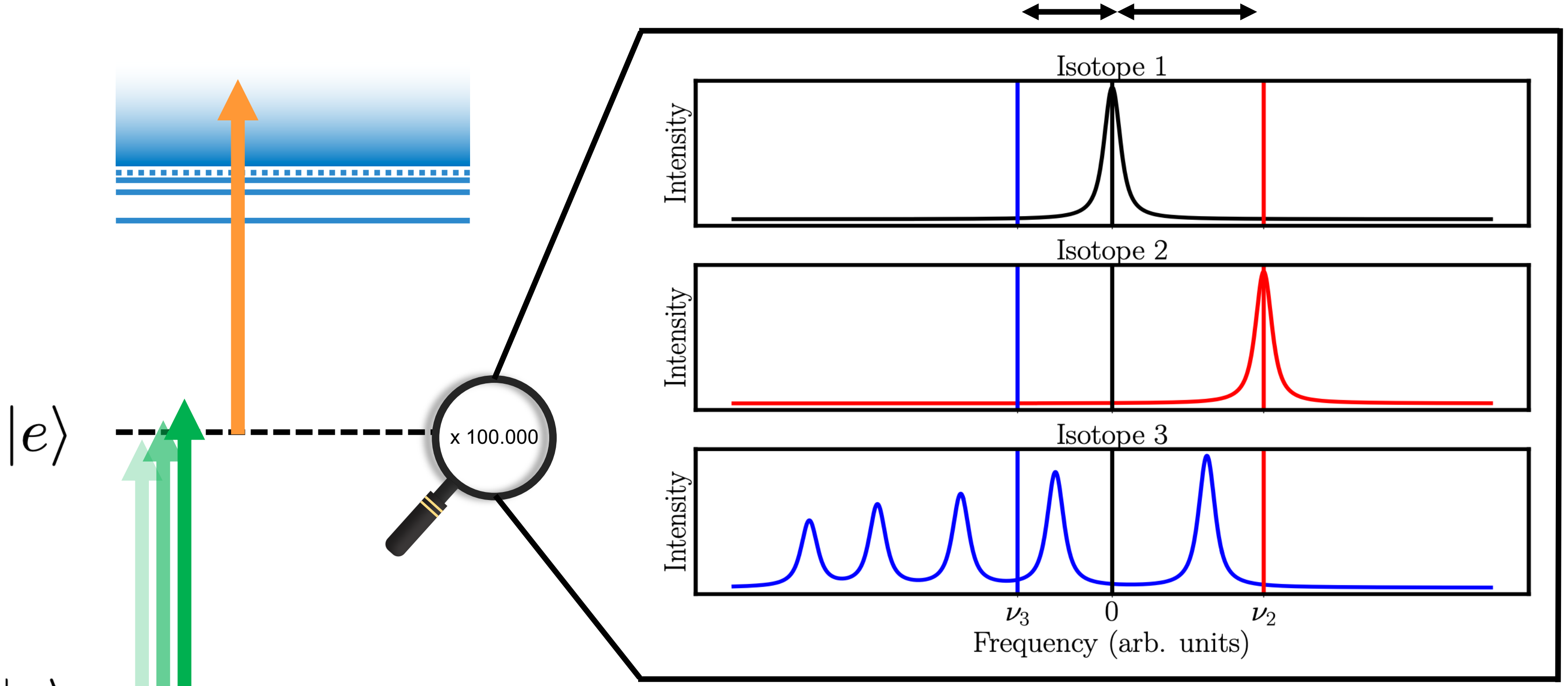

Isotope shift

Size

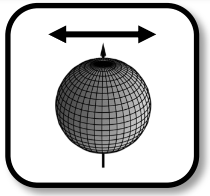

Hyperfine splitting

$$\mathcal{A} = \mu \frac{B_e(0)}{I \cdot J}$$

$$\mathcal{B} = eQ_S \left\langle \frac{\delta^2 V}{\delta z^2} \right\rangle$$

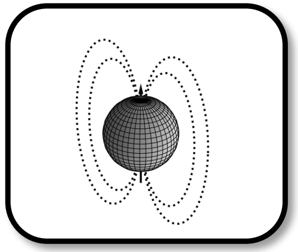

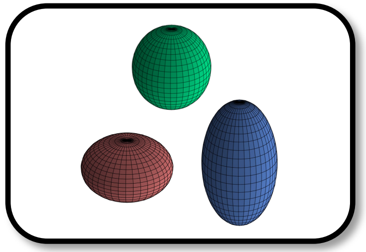

Electromagnetic moments can be derived in a nuclear-model-independent way

RESONANCE IONIZATION SPECTROSCOPY

TECHNISCHE UNIVERSITÄT DARMSTADT

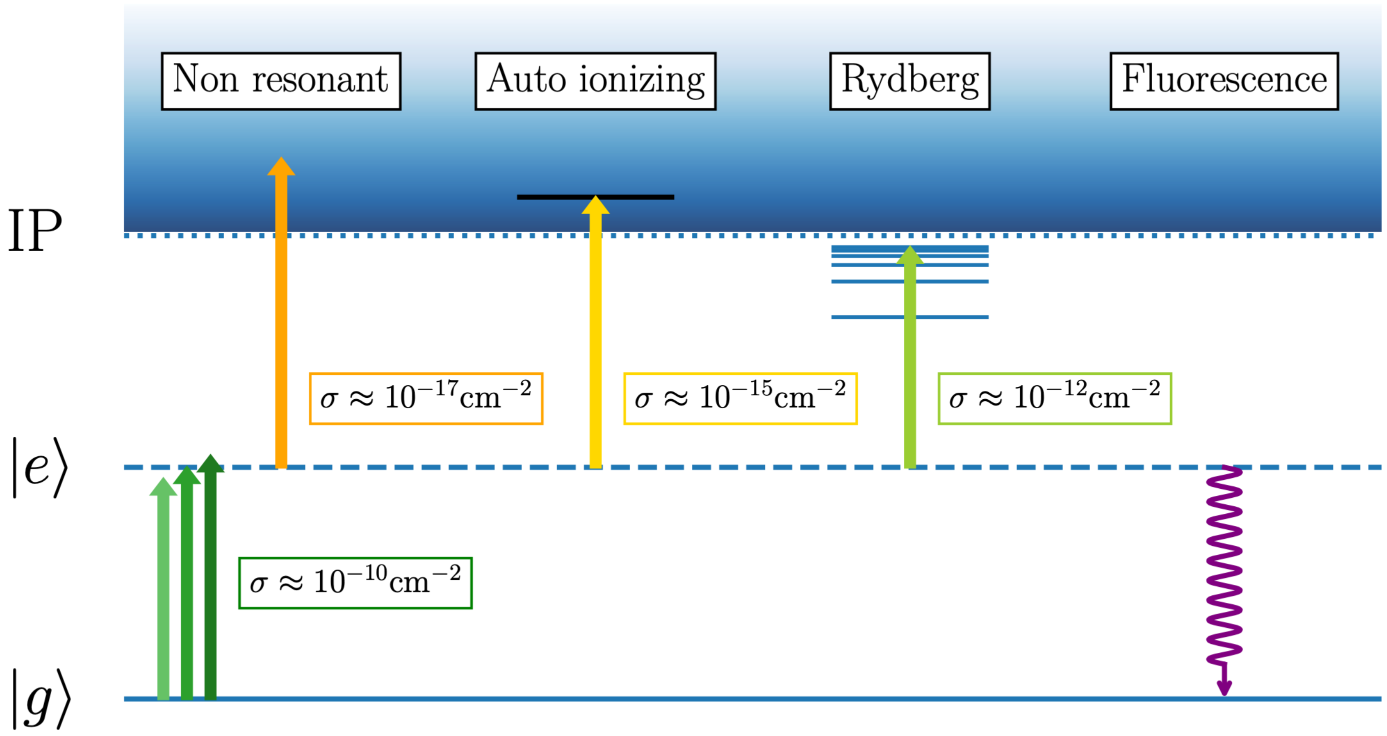

Non resonant: no knowledge about level scheme needed

AI: higher cross section than non-resonant excitation

Rydberg: can be used to determine ionization potential

Laser spectroscopy is a highly selective and efficient technique

RADIATION DETECTED RESONANCE IONIZATION SPECTROSCOPY (RADRIS)

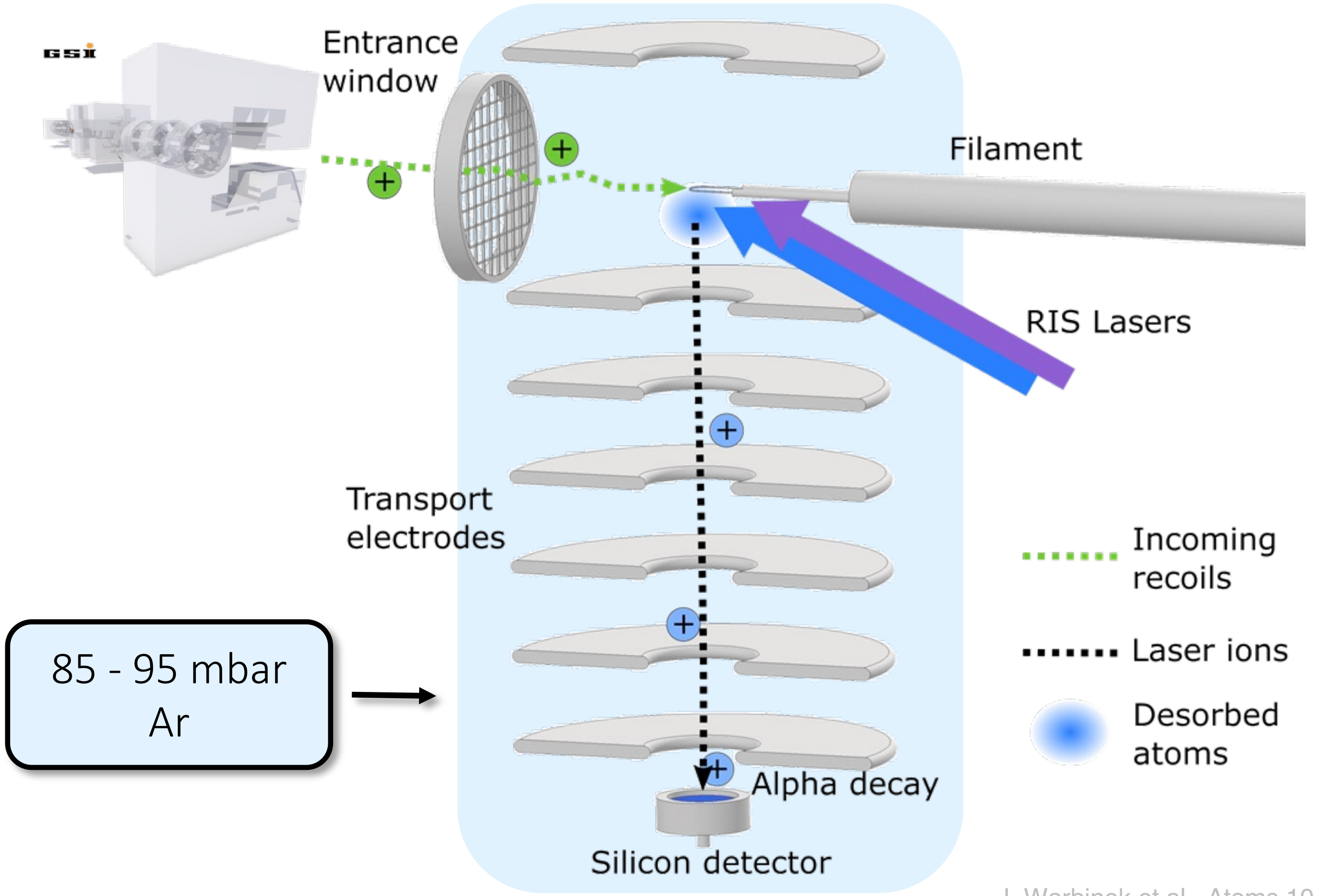

J. Warbinek et al., Atoms 10, 41 (2022)

Procedure:

1. Production and separation
2. Thermalizing incoming fusion products
3. Collection and neutralization on filament
4. Evaporation of neutral atoms
5. Two-step resonance laser ionization
6. Subsequent detection by α-decay

ISOTOPIC CHAIN IN CALIFORNIUM

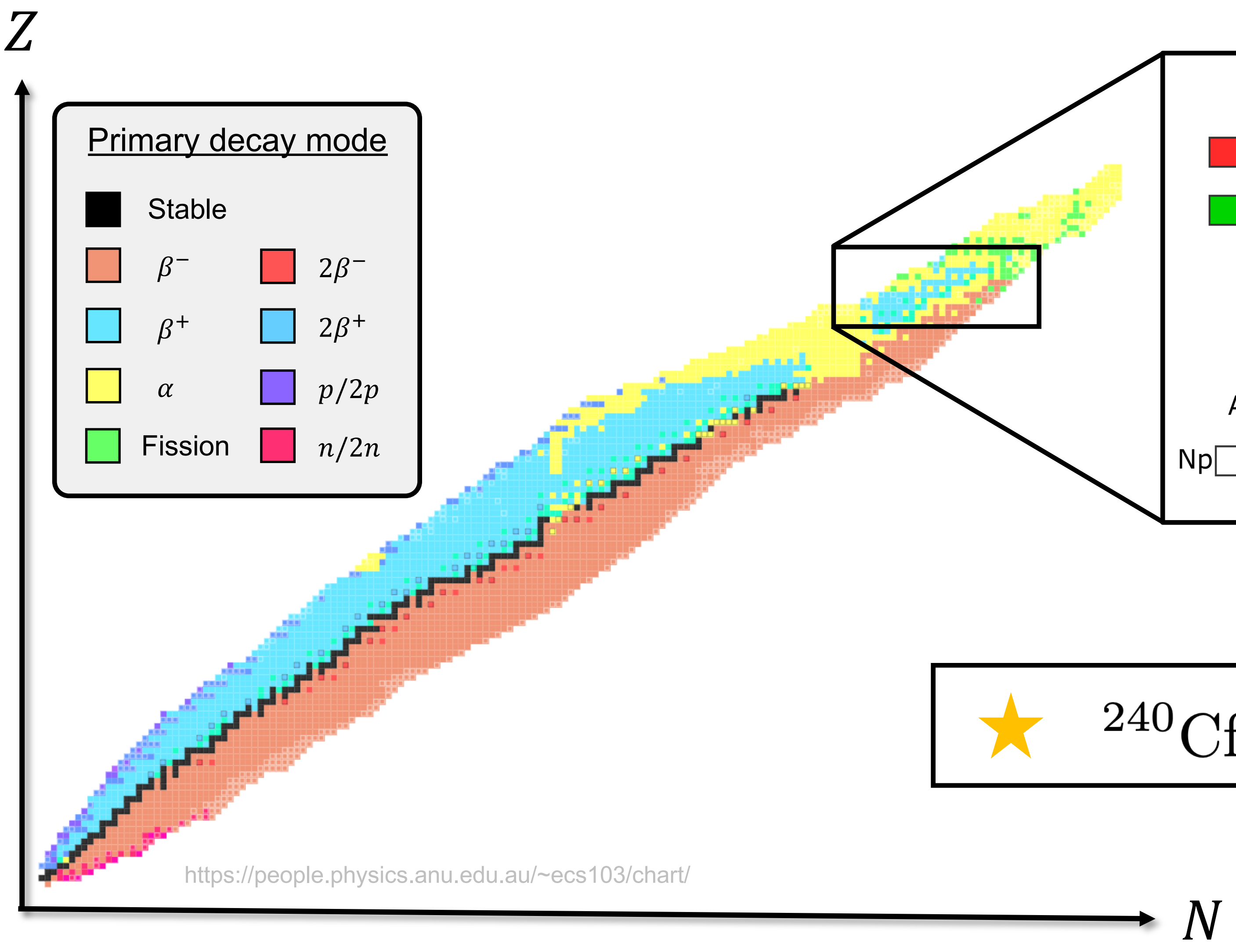

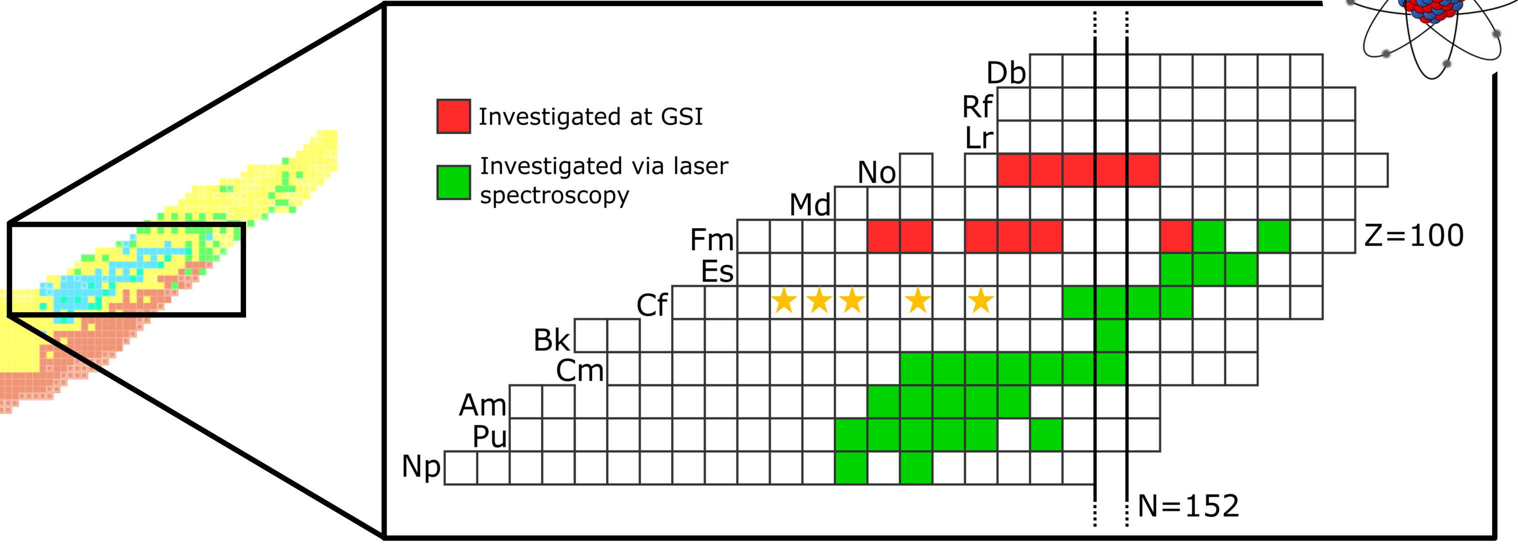

★ ^{240}Cf, ^{241}Cf, ^{242}Cf, ^{244}Cf, ^{246}Cf

PRODUCTION OF CALIFORNIUM AT GSI

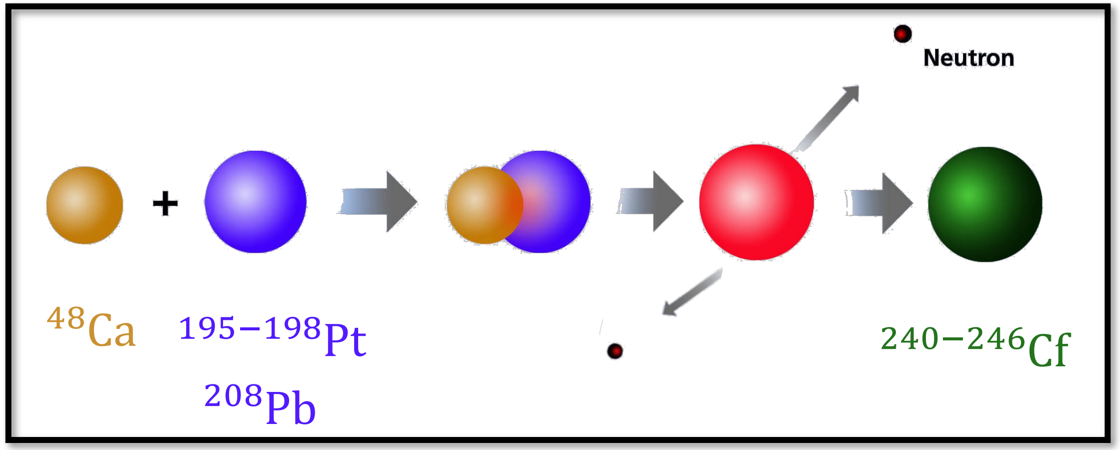

- Direct production of $^{240-244}\mathrm{Cf}$ with Pt
- Indirect production via $^{254}\mathrm{No}$ via subsequent α decays
- Long half-life challenging for RADRIS method

Isotope	Half-life	Reaction	Ions per hour
$^{240}\mathrm{Cf}$	0.96(15) min	$^{195}\mathrm{Pt}(^{48}\mathrm{Ca}, 3n)$	≈ 1
$^{241}\mathrm{Cf}$	3.78(70) min	$^{196}\mathrm{Pt}(^{48}\mathrm{Ca}, 3n)$	1 - 1.5
$^{242}\mathrm{Cf}$	3.5(2) min	$^{196}\mathrm{Pt}(^{48}\mathrm{Ca}, 2n)$	5 - 6
$^{244}\mathrm{Cf}$	19.4(6) min	$^{198}\mathrm{Pt}(^{48}\mathrm{Ca}, 2n)$	9 - 10
$^{246}\mathrm{Cf}$	35.7(5) h	$^{208}\mathrm{Pb}(^{48}\mathrm{Ca}, 2n)$ $^{254}\mathrm{No} \xrightarrow{\alpha,\alpha} {}^{246}\mathrm{Cf}$	18 - 22

ISOTOPE SHIFTS

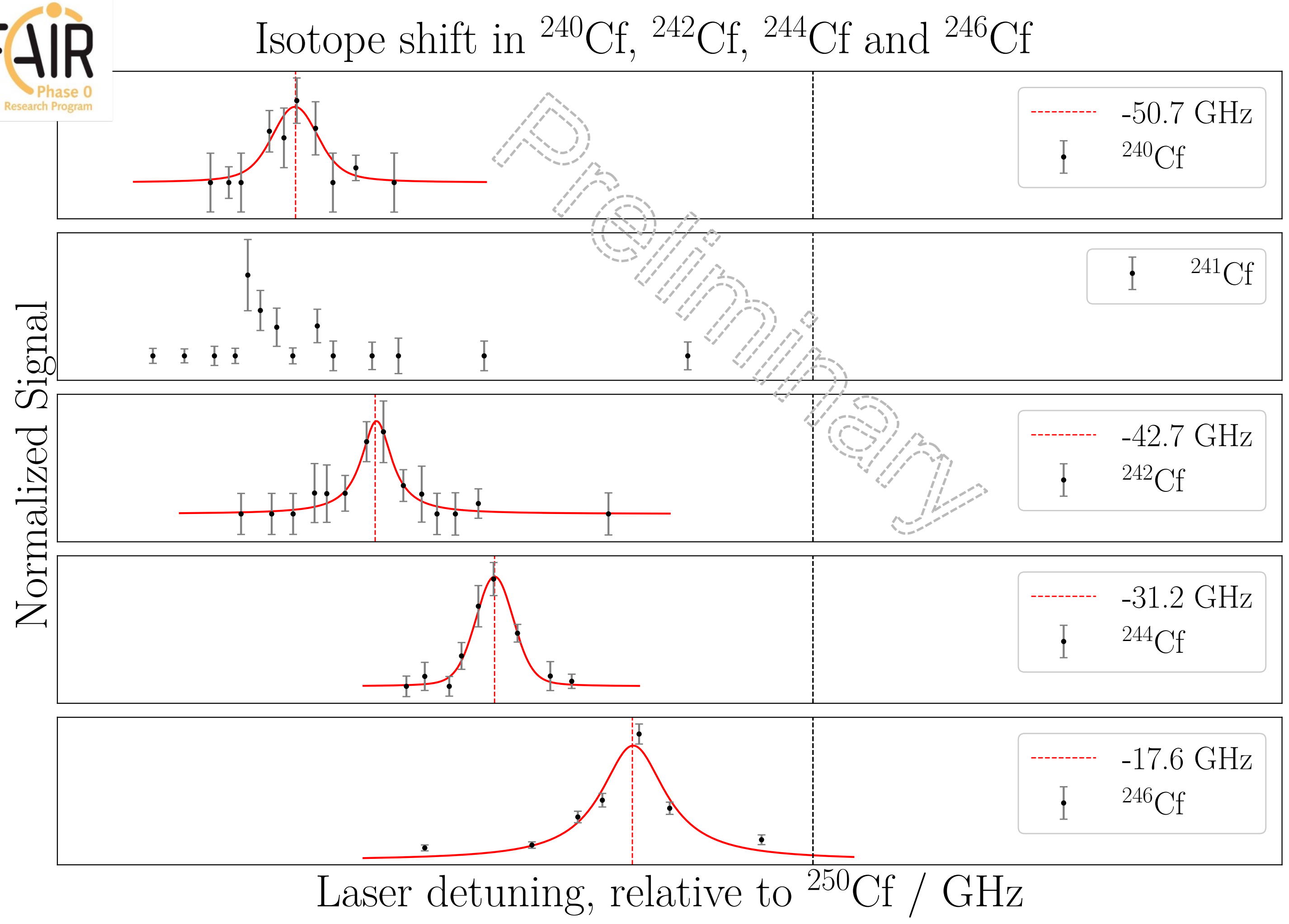

Reference Isotope

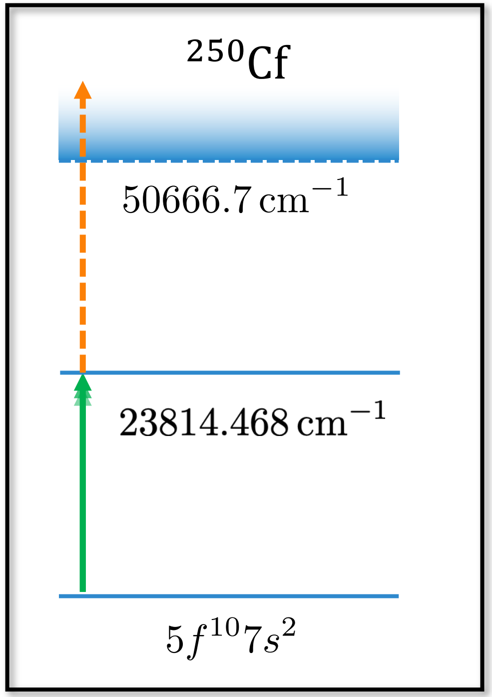

Weber et al. *Atoms* **2022**, *10*(2), 51

TECHNISCHE UNIVERSITÄT DARMSTADT

FROM ISOTOPE SHIFT TO CHANGES IN MEAN-SQUARE CHARGE RADII

Weber et al. *Atoms* **2022**, *10*(2), 51

$$\delta\langle r^2\rangle^{A,A'} = \left(\delta\nu^{A,A'} - \frac{K}{\mu}\right)\cdot\frac{1}{F}$$

Input from atomic theory (CI, MCDHF,...)

High uncertainty due to large number if open f-shells in the actinides

$$F_{420} = 91(27)\,\mathrm{GHz/fm^2}$$

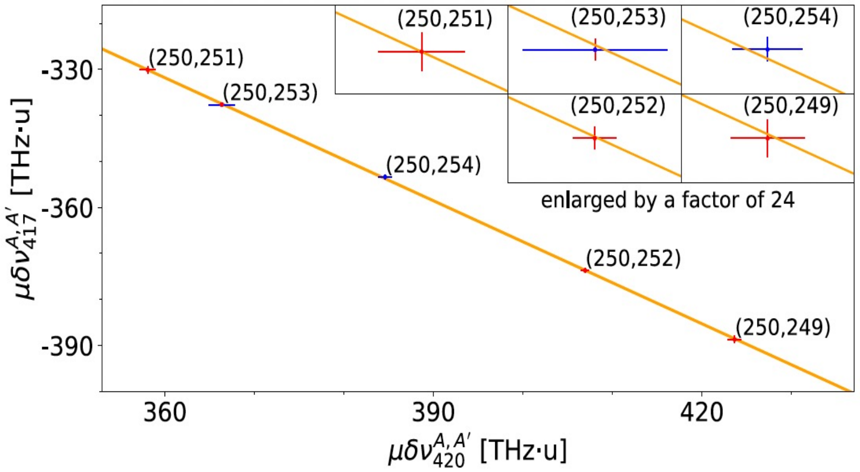

$$\mu\cdot\delta\nu_i^{A,A'} = \underbrace{\mu\cdot\frac{\mathrm{F}_i}{\mathrm{F}_j}}_{\text{slope}}\cdot\delta\nu_j^{A,A'}\underbrace{-\frac{\mathrm{F}_i}{\mathrm{F}_j}\cdot\mathrm{K}_j+\mathrm{K}_i}_{\text{intercept}}$$

$$\frac{F_{417}}{F_{420}} = -0.891(6)$$

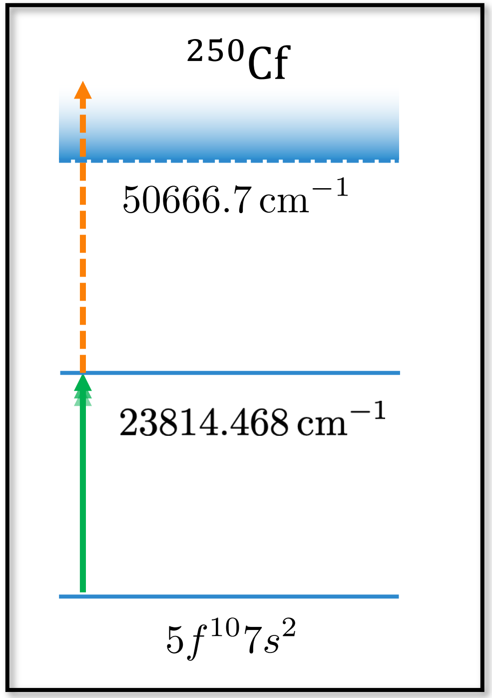

$$F_{420} = 91(9)\,\mathrm{GHz/fm^2}$$

FROM ISOTOPE SHIFT TO CHANGES IN MEAN-SQUARE CHARGE RADII

- Mostly smooth isotope-shift evolution, with no large universal kink established at $N = 152$
- Bulk size is less sensitive to the subshell closure
- Similar trend as recently established in an isotopic chain on fermium

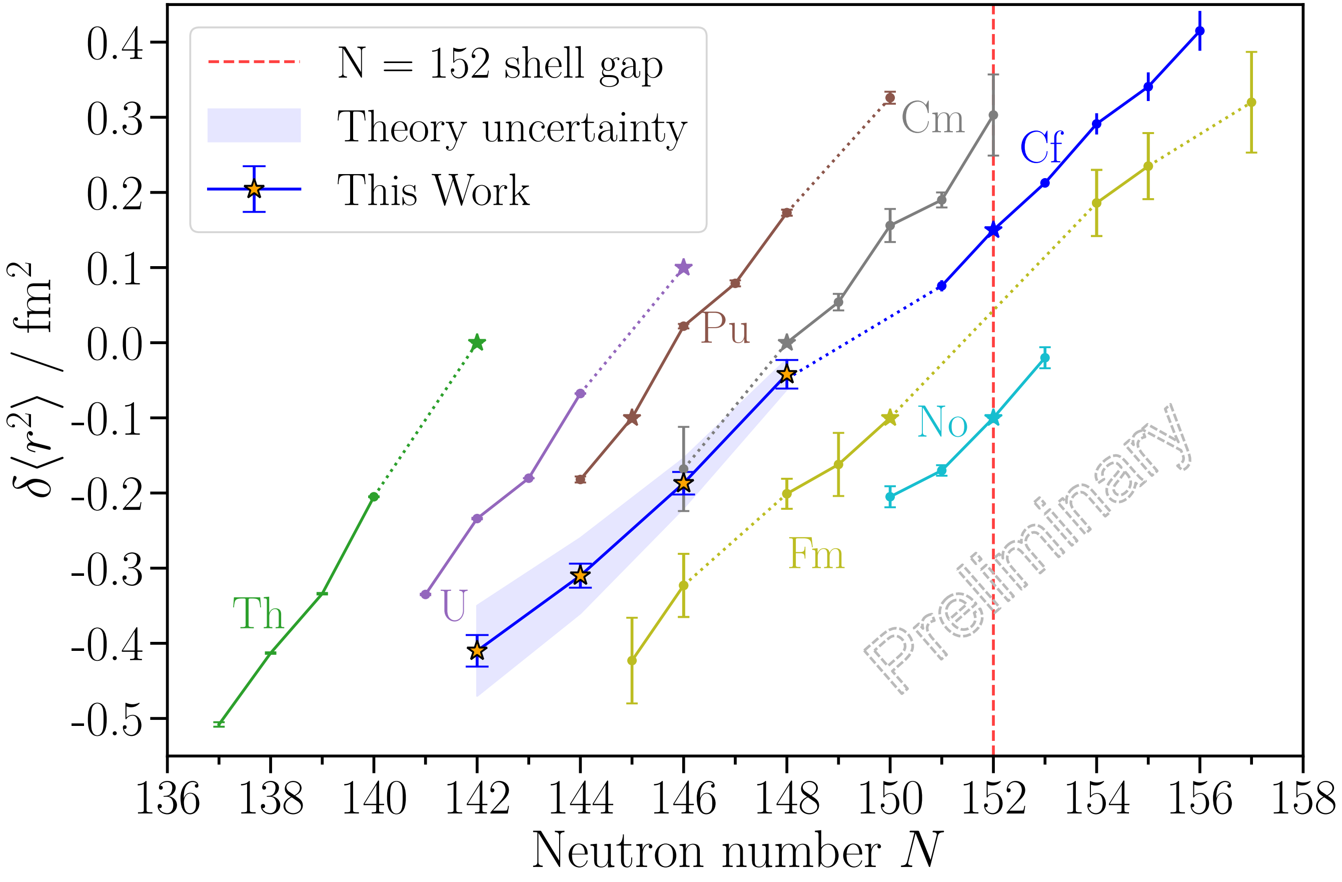

FROM ISOTOPE SHIFT TO CHANGES IN MEAN-SQUARE CHARGE RADII

- Mostly smooth isotope-shift evolution, with no large universal kink established at $N = 152$
- Bulk size is less sensitive to the subshell closure
- Similar trend as recently established in an isotopic chain on fermium

Article

Smooth trends in fermium charge radii and the impact of shell effects

https://doi.org/10.1038/s41586-024-08062-z

Received: 20 December 2023

Accepted: 17 September 2024

Published online: 30 October 2024

Open access

Check for updates

Jessica Warbinek[1,2,3,28]✉, Elisabeth Rickert[1,2,3], Sebastian Raeder[1,3]✉, Thomas Albrecht-Schönzart[4], Brankica Andelic[1,3,5], Julian Auler[2], Benjamin Bally[6], Michael Bender[7], Sebastian Berndt[2], Michael Block[1,2,3], Alexandre Brizard[8], Pierre Chauveau[1,3], Bradley Cheal[9], Premaditya Chhetri[1,3,10], Arno Claessens[10], Antoine de Roubin[10], Charlie Devlin[9], Holger Dorrer[2], Christoph E. Düllmann[1,2,3], Julie Ezold[11], Rafael Ferrer[10], Vadim Gadelshin[12], Alyssa Gaiser[13,14], Francesca Giacoppo[1,3], Stephane Goriely[15], Manuel J. Gutiérrez[1,3], Ashley Harvey[11], Raphael Hasse[12], Reinhard Heinke[12], Fritz-Peter Heßberger[1], Stephane Hilaire[16,17], Magdalena Kaja[12], Oliver Kaleja[1,18], Tom Kieck[1,2,3], EunKang Kim[2], Nina Kneip[12], Ulli Köster[19], Sandro Kraemer[10], Mustapha Laatiaoui[2], Jeremy Lantis[2], Nathalie Lecesne[8], Andrea Tzeitel Loria Basto[2,3], Andrew Kishor Mistry[1,20,21], Christoph Mokry[2,3], Iain Moore[22], Tobias Murböck[1,3], Danny Münzberg[1,2,3], Witold Nazarewicz[13,23], Thorben Niemeyer[12], Steven Nothhelfer[1,2,3], Sophie Péru[16,17], Andrea Raggio[22], Paul-Gerhard Reinhard[24], Dennis Renisch[2,3], Emmanuel Rey-Herme[25], Jekabs Romans[10], Elisa Romero Romero[2], Jörg Runke[1,2], Wouter Ryssens[15], Hervé Savajols[8], Fabian Schneider[2], Joseph Sperling[4], Matou Stemmler[12], Dominik Studer[1,3,12], Petra Thörle-Pospiech[2,3], Norbert Trautmann[2], Mitzi Urquiza-González[26,27], Kenneth van Beek[21], Shelley Van Cleve[11], Piet Van Duppen[10], Marine Vandebrouck[25], Elise Verstraelen[10], Thomas Walther[21], Felix Weber[12] & Klaus Wendt[12]

TECHNISCHE UNIVERSITÄT DARMSTADT

SUMMARY AND OUTLOOK

- Isotopic shifts and changes in rms charge radii were determined for even-even Cf isotopes: $^{240}\mathrm{Cf}$, $^{242}\mathrm{Cf}$, $^{244}\mathrm{Cf}$ and $^{246}\mathrm{Cf}$

- Smooth trend for charge radii continue to show up in the heavy actinide region
  - Collective behavior masks single particle effects that impact the charge radius

- Long-lived $^{252}\mathrm{Fm}$ (25.4h) on the deformed subshell closures $N = 152$ and $Z = 100$ now in range for the RADRIS technique

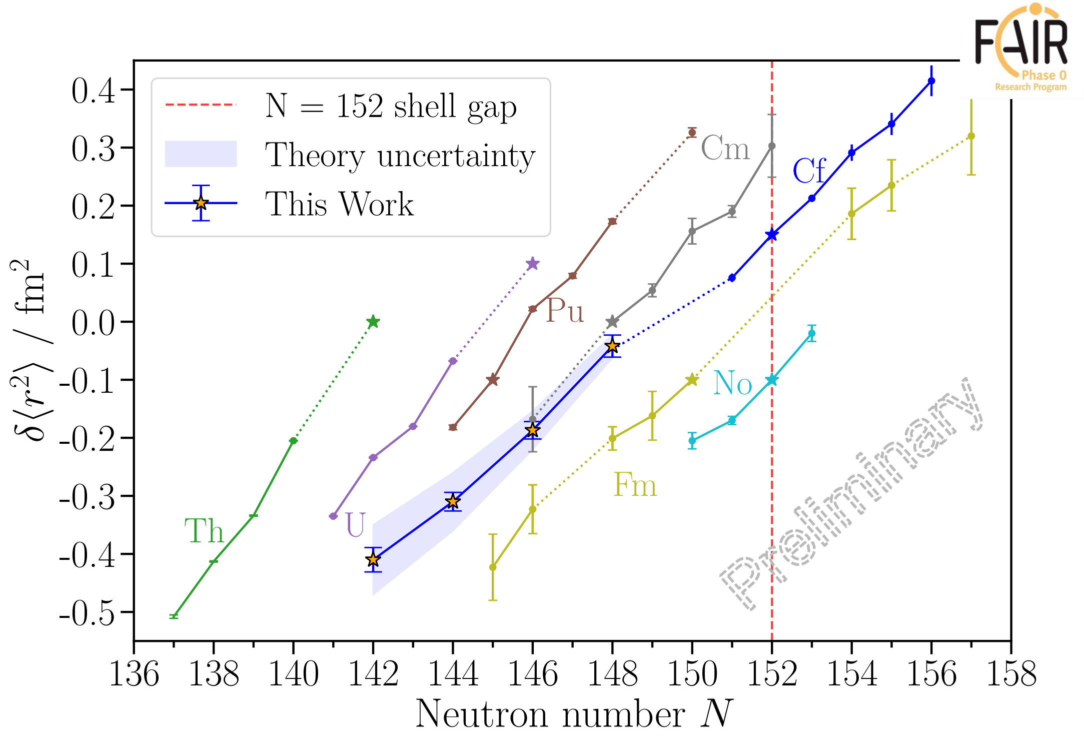

TECHNISCHE UNIVERSITÄT DARMSTADT

GSI Darmstadt

M. Block, F. Giacoppo, F.P. Heßberger, A. Mistry, S. Raeder, J. Warbinek, A.Yakushev, B. Hartigan, M. Gutiérrez-Torres,

KU Leuven

A. Claessens, R. Ferrer, S. Kraemer, P. Van Duppen, F. Ivandikov, Harshithbabu

Universität Mainz

Ch. E. Düllmann, M. Stemmler, K Wendt, S. Berndt, Th. Niemeyer, R. Hasse, P. Chhetri,

TU Darmstadt

Th. Walther, K. van Beek

RUG Groningen

T. Van de Vendel, J. Even

Helmholtz Institut Mainz

D. Münzberg, E. Rickert, T. Kieck, D. Studer, J. Hindermann, J. Weyrich

GANIL / LPC Caen / Orsay

N. Lecesne, A. Lopez, V. Marchant, H. Savajols, V. Manea, A. Brizard, S. Geldhof, A. De Roubin, E. Morin, D. Ackermann, M. Laatiaoui,

TRIUMF Vancouver

P. Kunz

University of Granada

D. Rodriguez

University of Jyväskylä

A. Raggio

THANK YOU FOR YOUR ATTENTION !

Bundesministerium für Forschung, Technologie und Raumfahrt

GSI

FAIR Phase 0 Research Program

HIM HELMHOLTZ Helmholtz-Institut Mainz

JG|U JOHANNES GUTENBERG UNIVERSITÄT MAINZ

KU LEUVEN

university of groningen

UNIVERSITY OF JYVÄSKYLÄ

cea PARIS-SACLAY

LISA LASER IONISATION AND SPECTROSCOPY OF ACTINIDES

GANIL

This Marie Sklodowska-Curie Action (MSCA) Innovative Training Network (ITN) receives funding from the European Union H2020 Framework Programme under grant agreement no. 861198.

SHELL EFFECT SENSITIVE QUANTITIES

- B(E2) values
- $E(2_1^+)$
- Spacing in rotational bands
- Q_α
- Half-lives
- Hindrance factors
- ….

M. Block / Nuclear Physics A 944 (2015) 471–491

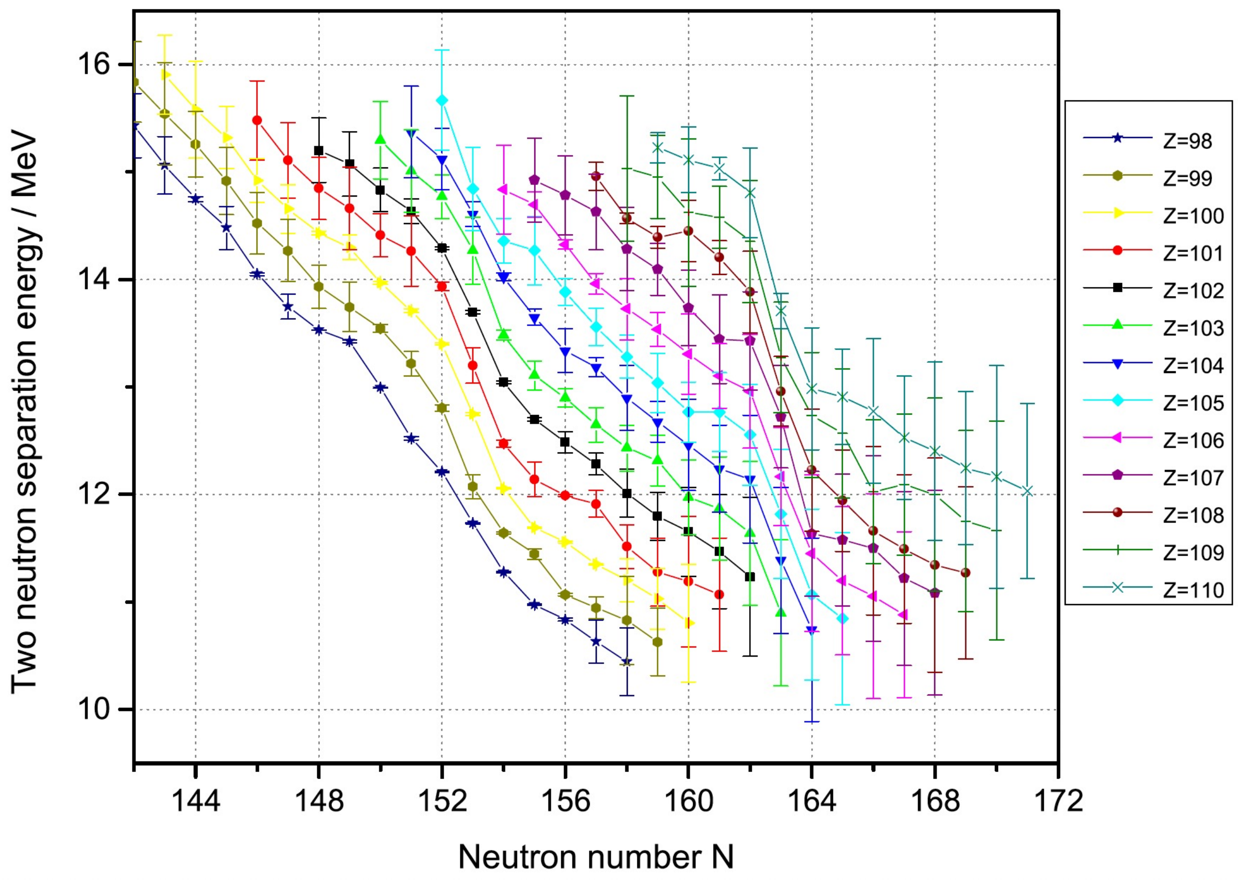

PRODUCING HEAVY ELEMENTS

TECHNISCHE UNIVERSITÄT DARMSTADT

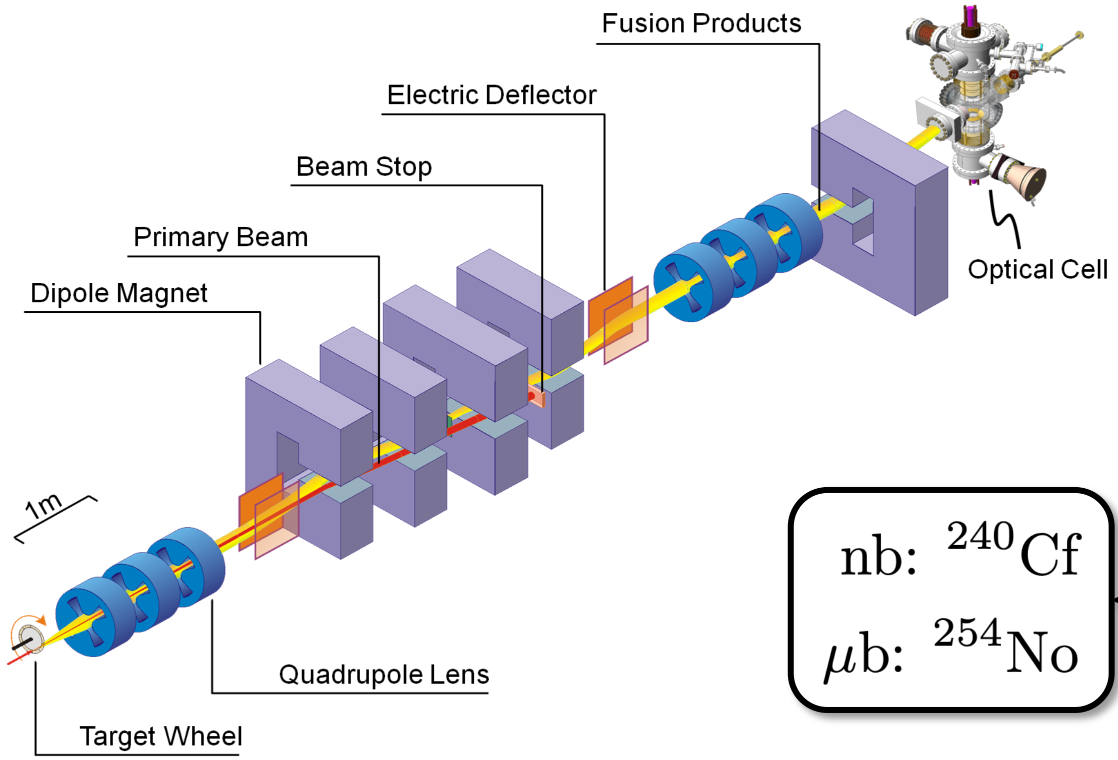

H. Backe, W. Lauth, M. Block, M. Laatiaoui, , Nuclear Physics A, (2015)

Impinge rotating target wheel with beam

$I_{\mathrm{Beam}} \approx 10^{12}/s$

$E_{\mathrm{Beam}} \approx 4 - 5\,\mathrm{MeV/u}$

Fusion-evaporation reaction

$\sigma_{\mathrm{Prod.}} = \mathrm{nb} - \mathrm{mb}$

nb: $^{240}\mathrm{Cf}$

μb: $^{254}\mathrm{No}$

Separating compound nuclei from primary beam

$v = \frac{E}{B}$

Injection into setup

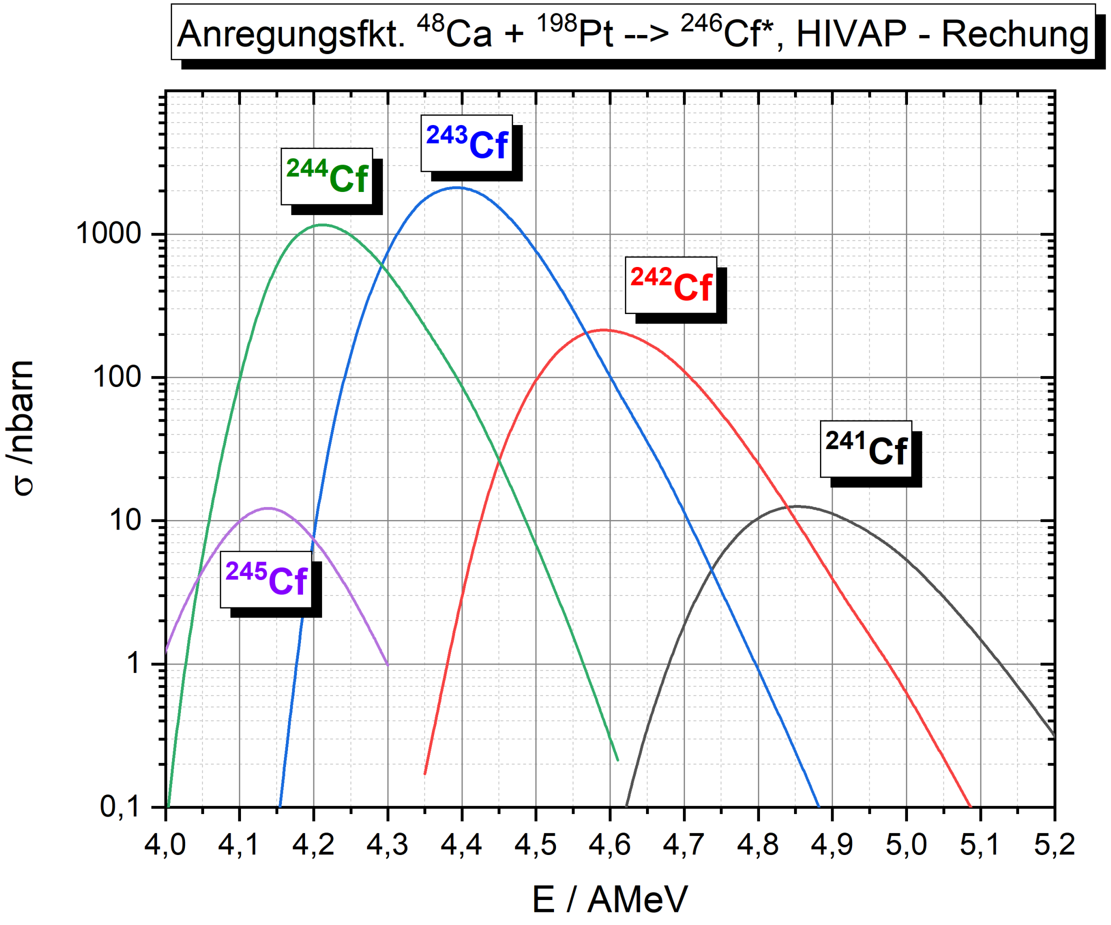
Anregungsfkt. 48Ca + 198Pt --> 246Cf*, HIVAP - Rechung
244Cf
243Cf
242Cf
241Cf
245Cf
σ /nbarn
1000
100
10
1
0,1
4,0 4,1 4,2 4,3 4,4 4,5 4,6 4,7 4,8 4,9 5,0 5,1 5,2
E / AMeV

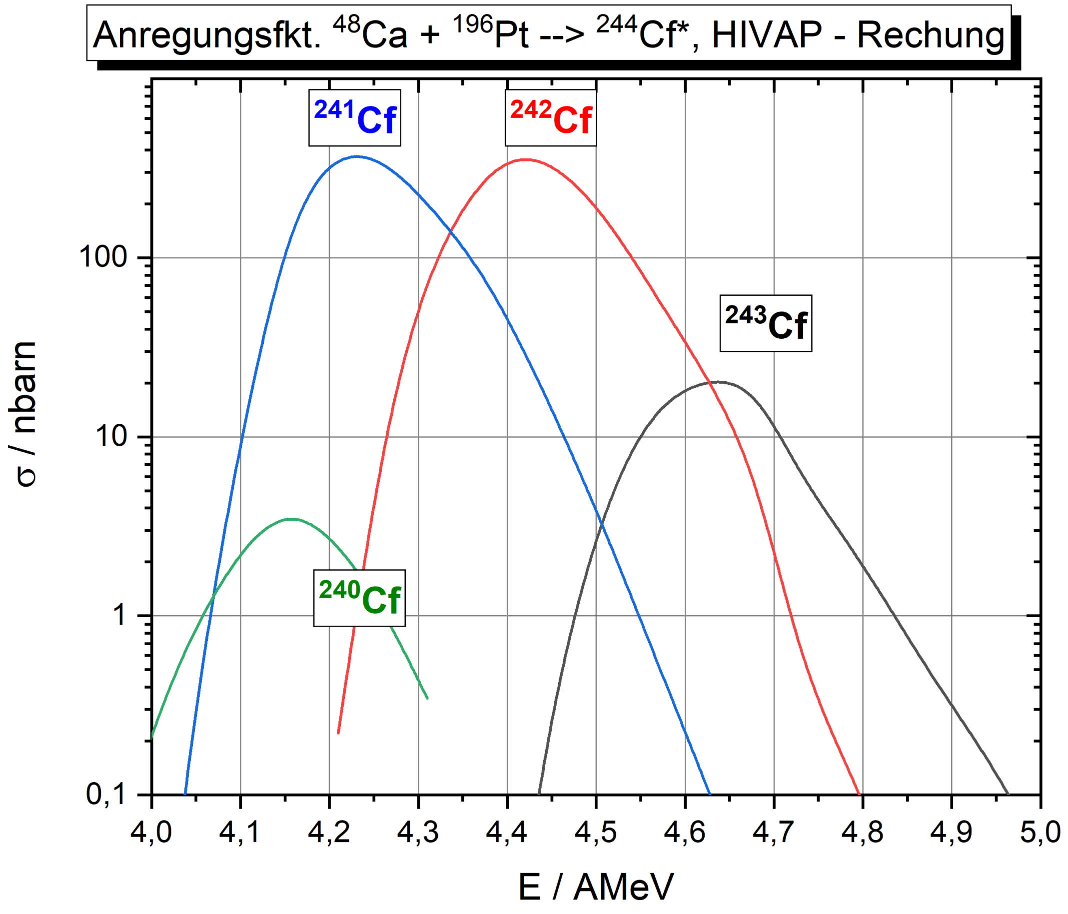
Anregungsfkt. 48Ca + 196Pt --> 244Cf*, HIVAP - Rechung
241Cf
242Cf
243Cf
240Cf
σ / nbarn
100
10
1
0,1
4,0 4,1 4,2 4,3 4,4 4,5 4,6 4,7 4,8 4,9 5,0
E / AMeV

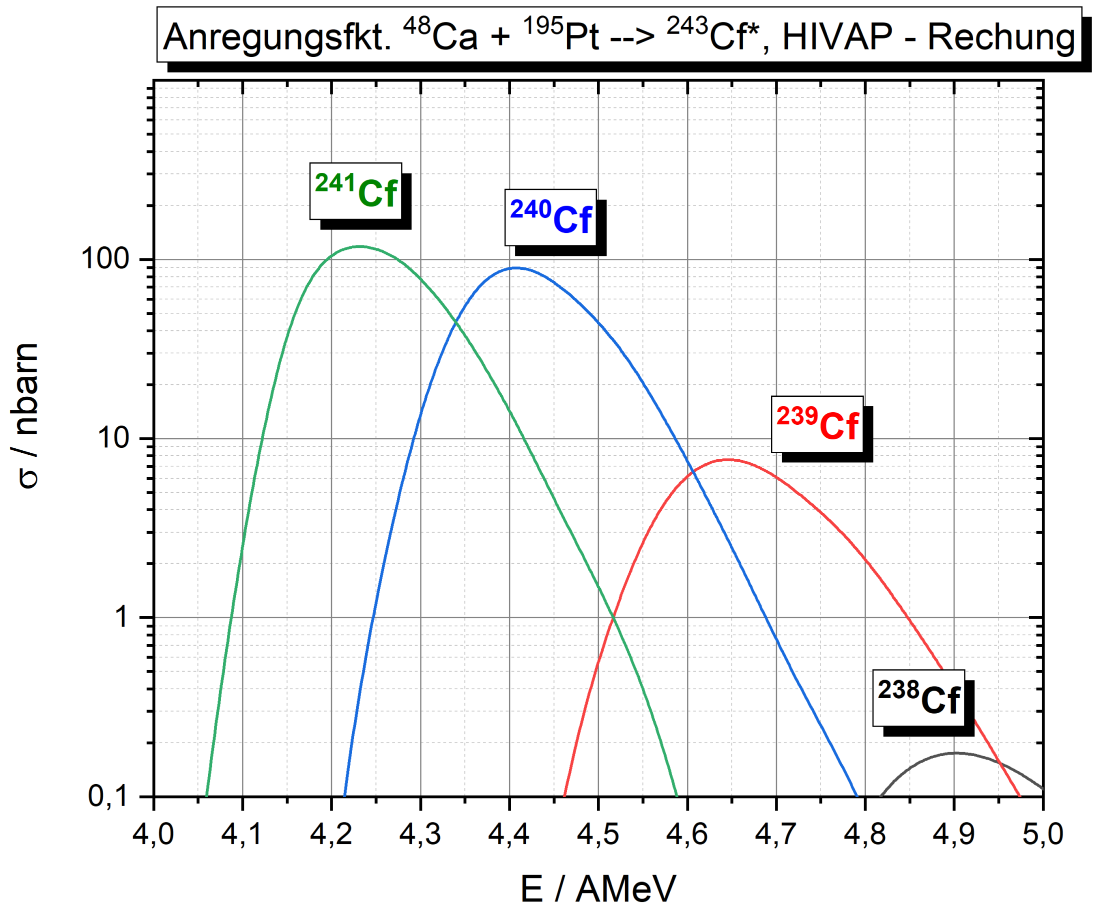
Anregungsfkt. 48Ca + 195Pt --> 243Cf*, HIVAP - Rechung
241Cf
240Cf
239Cf
238Cf
σ / nbarn
100
10
1
0,1
4,0
4,1
4,2
4,3
4,4
4,5
4,6
4,7
4,8
4,9
5,0
E / AMeV

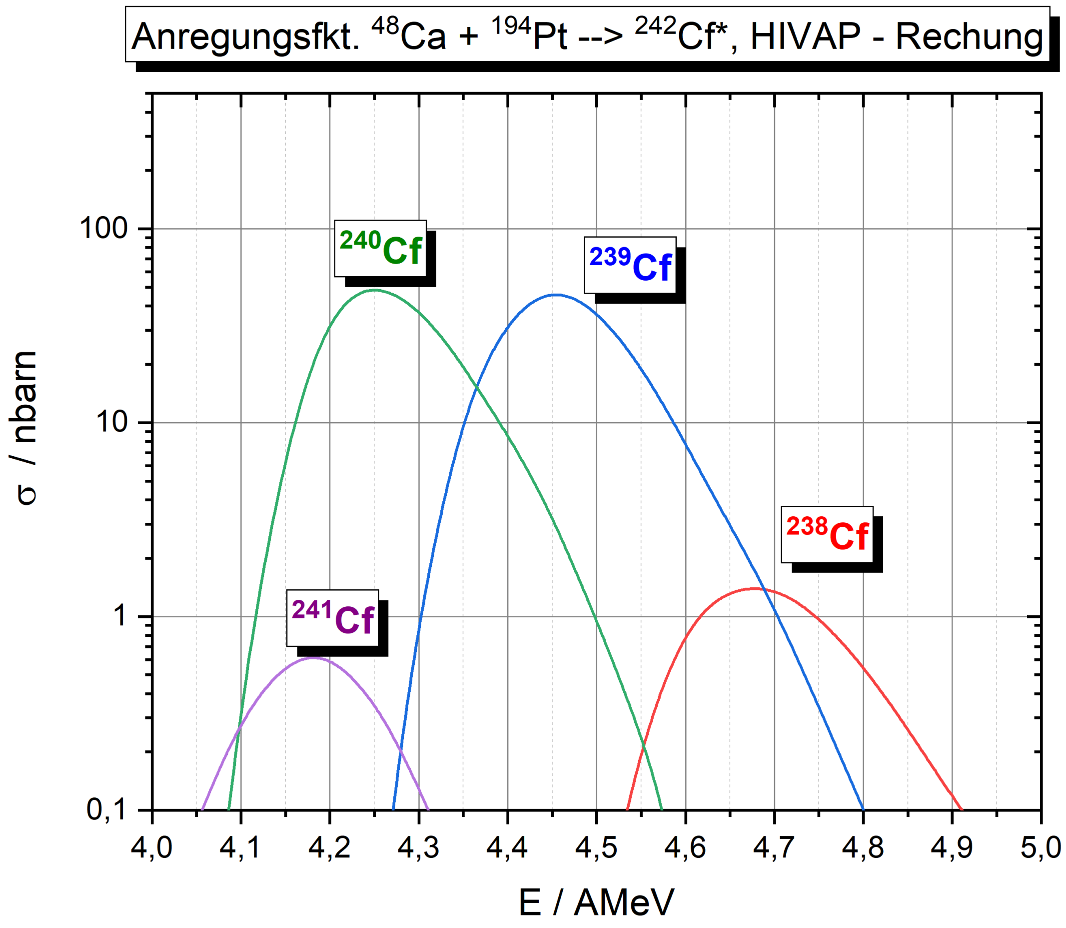
Anregungsfkt. 48Ca + 194Pt --> 242Cf*, HIVAP - Rechung
240Cf
239Cf
241Cf
238Cf
σ / nbarn
100
10
1
0,1
4,0
4,1
4,2
4,3
4,4
4,5
4,6
4,7
4,8
4,9
5,0
E / AMeV

TECHNISCHE UNIVERSITÄT DARMSTADT

LONG HALF-LIVES: A CHALLENGE FOR RADRIS

Three rotatable detectors

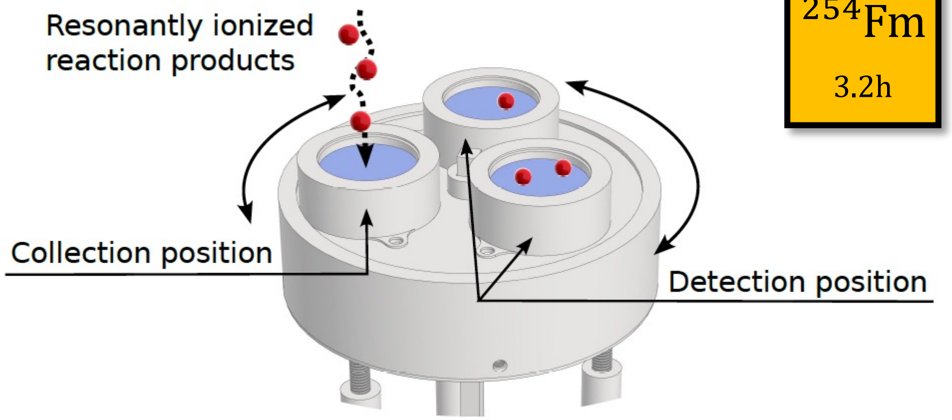

^{254}Fm

3.2h

Access to longer-lived nuclei

Array of eight detectors

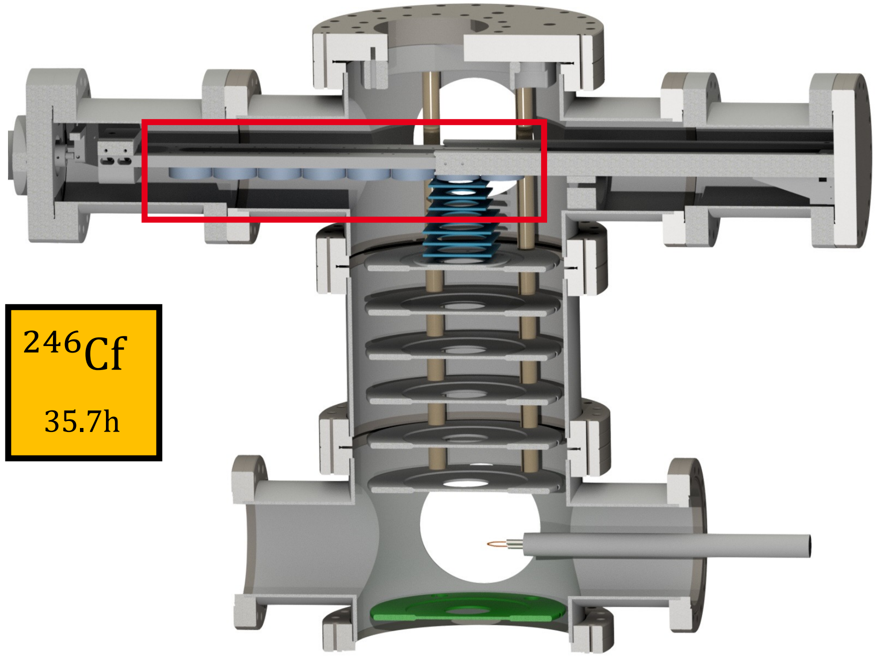

^{246}Cf

35.7h

PHYSICS OF HEAVY ELEMENTS

Nilsson model

Mean-field potential

$$V(\rho, z) = \frac{1}{2} m \left(\omega^2 \rho^2 + \omega_z^2 z^2\right)$$

Quantum Numbers

$$\Lambda, \Sigma, \Omega, K$$

States

$$\Omega^\pi \left[N, n_z, \Lambda\right]$$

Deformation

$$\delta = \frac{\Delta r}{\sqrt{\langle r^2 \rangle}} \approx \frac{3}{2}\sqrt{\frac{5}{4\pi}}\beta_2$$

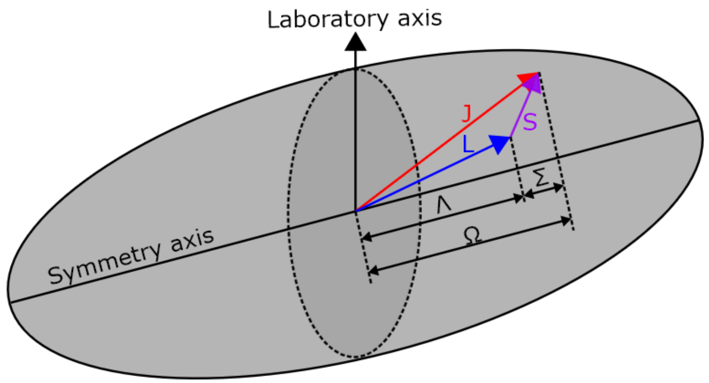

Nilsson label

$$7/2^- [514]$$

How do orbitals evolve with deformation?

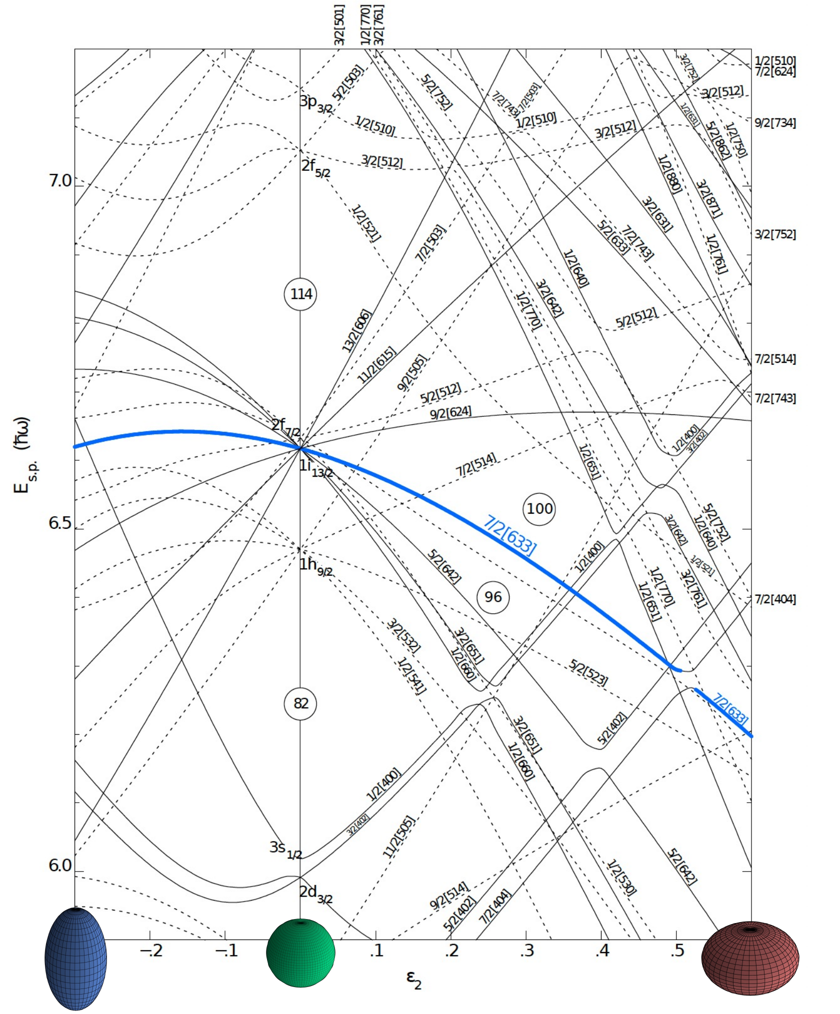

$$\epsilon_2 = \delta + \frac{1}{6}\delta^2 + \frac{5}{18}\delta^3 + \ldots$$

CYCLE FOR CALIFORNIUM 246

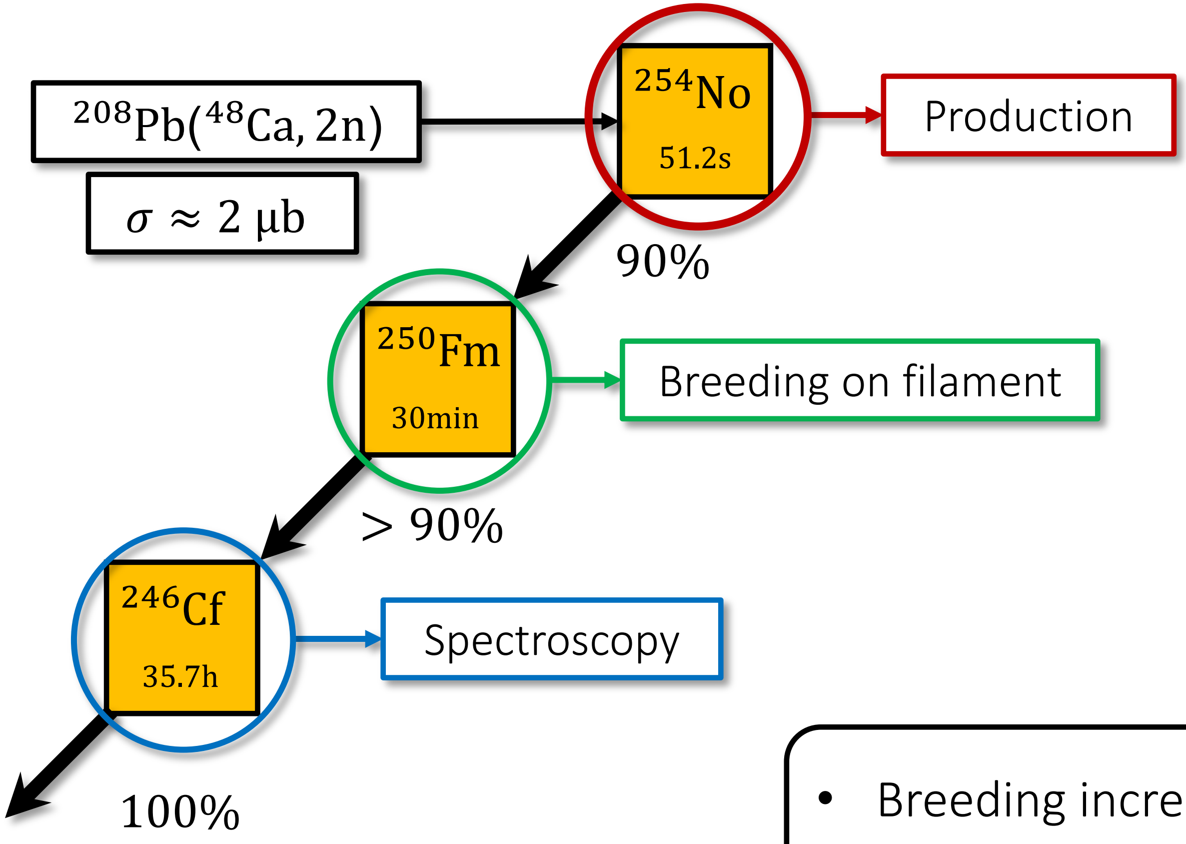

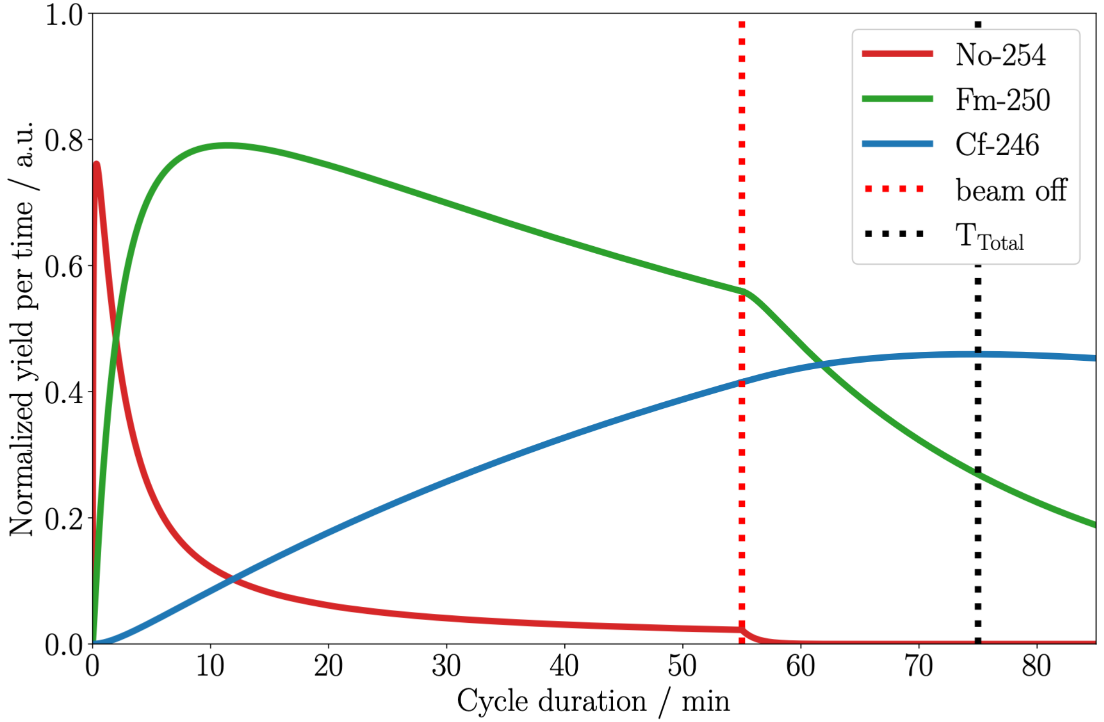

- Breeding increases Cf yield and decreases possible background from Fm
- Prolonging cycle past 75 min doesn't significantly increase gain

TECHNISCHE UNIVERSITÄT DARMSTADT

CYCLE FOR CALIFORNIUM 246

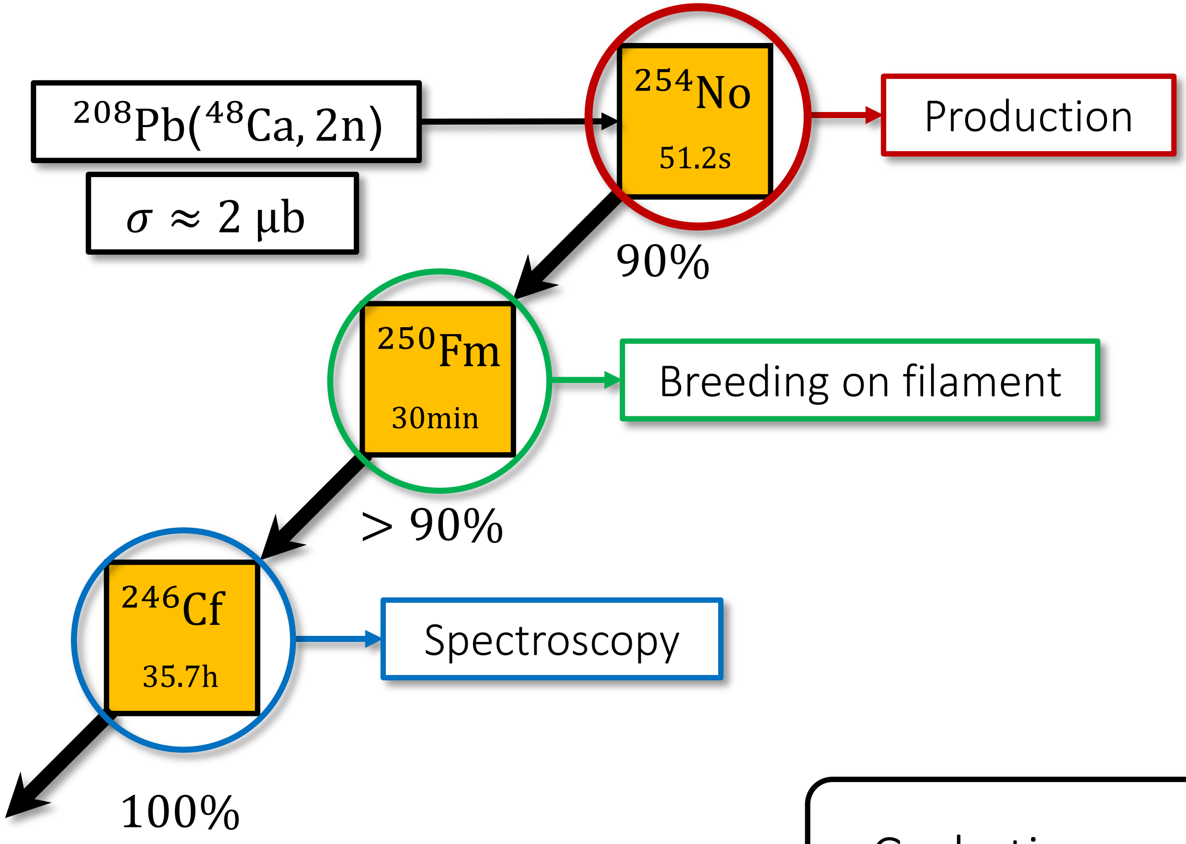

$$\dot{N}_{\mathrm{No}} = N_{\mathrm{Prod}} - \lambda_{\mathrm{No}} N_{\mathrm{No}}$$

$$\dot{N}_{\mathrm{Fm}} = \lambda_{\mathrm{No}} N_{\mathrm{No}} - \lambda_{\mathrm{Fm}} N_{\mathrm{Fm}}$$

$$\dot{N}_{\mathrm{Cf}} = \lambda_{\mathrm{Fm}} N_{\mathrm{Fm}} - \lambda_{\mathrm{Cf}} N_{\mathrm{Cf}}$$

$$N_{\mathrm{No}}(0) = N_{\mathrm{Cf}}(0) = N_{\mathrm{Fm}}(0) = 0$$

Cycle time optimized based on half-life of nuclide of interest

TECHNISCHE UNIVERSITÄT DARMSTADT

CYCLE FOR CALIFORNIUM 246

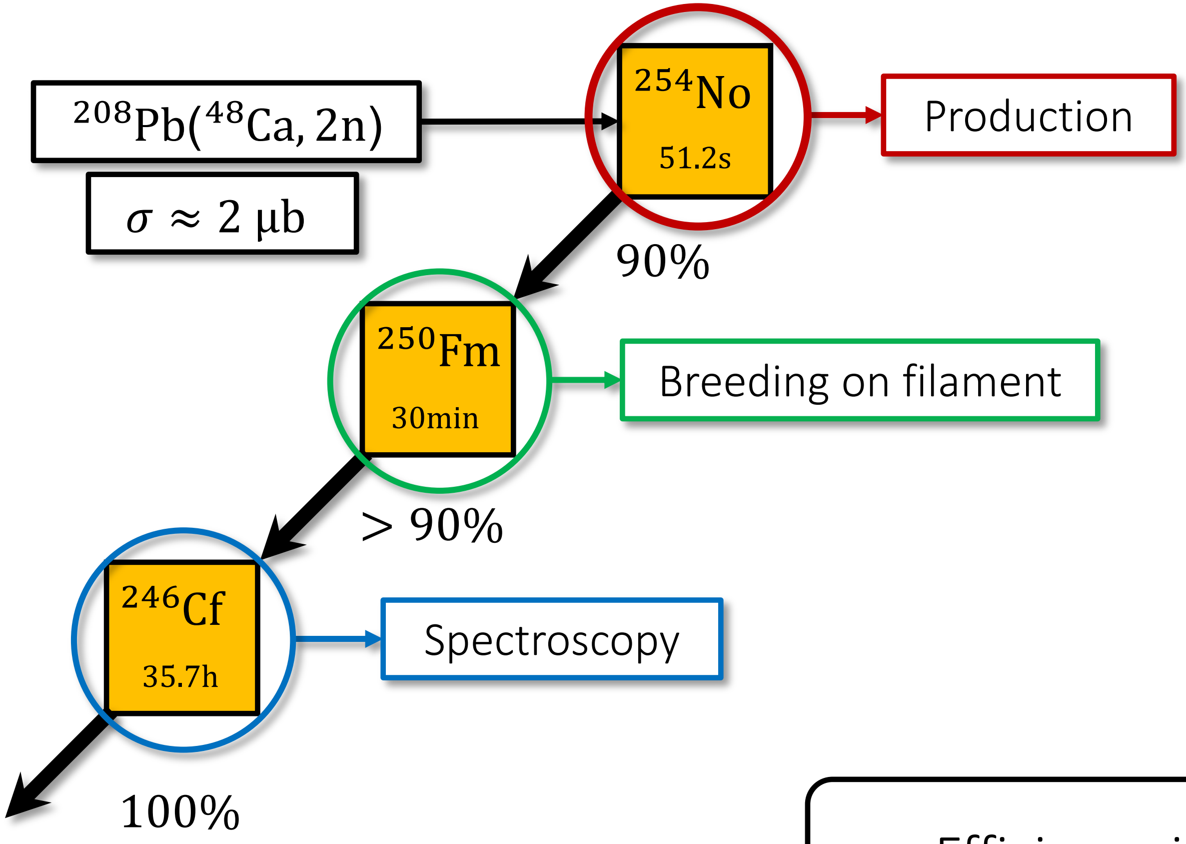

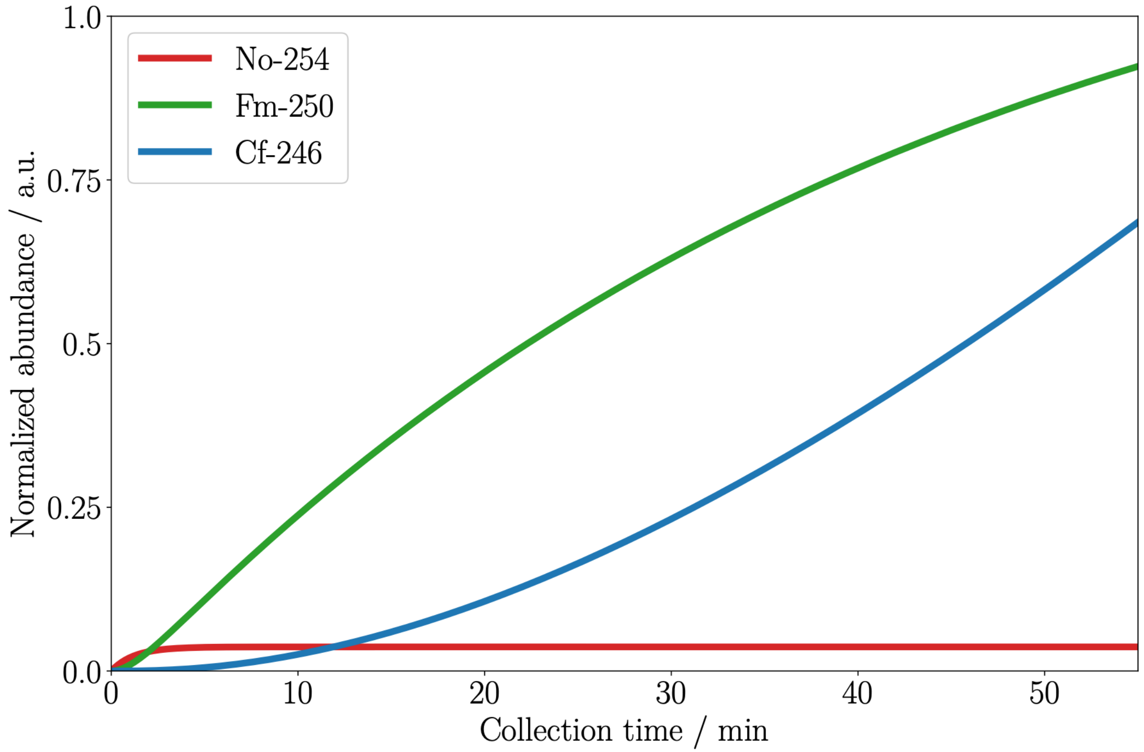

Efficiency is given by normalizing abundance over time

TECHNISCHE UNIVERSITÄT DARMSTADT

CYCLE FOR CALIFORNIUM 246

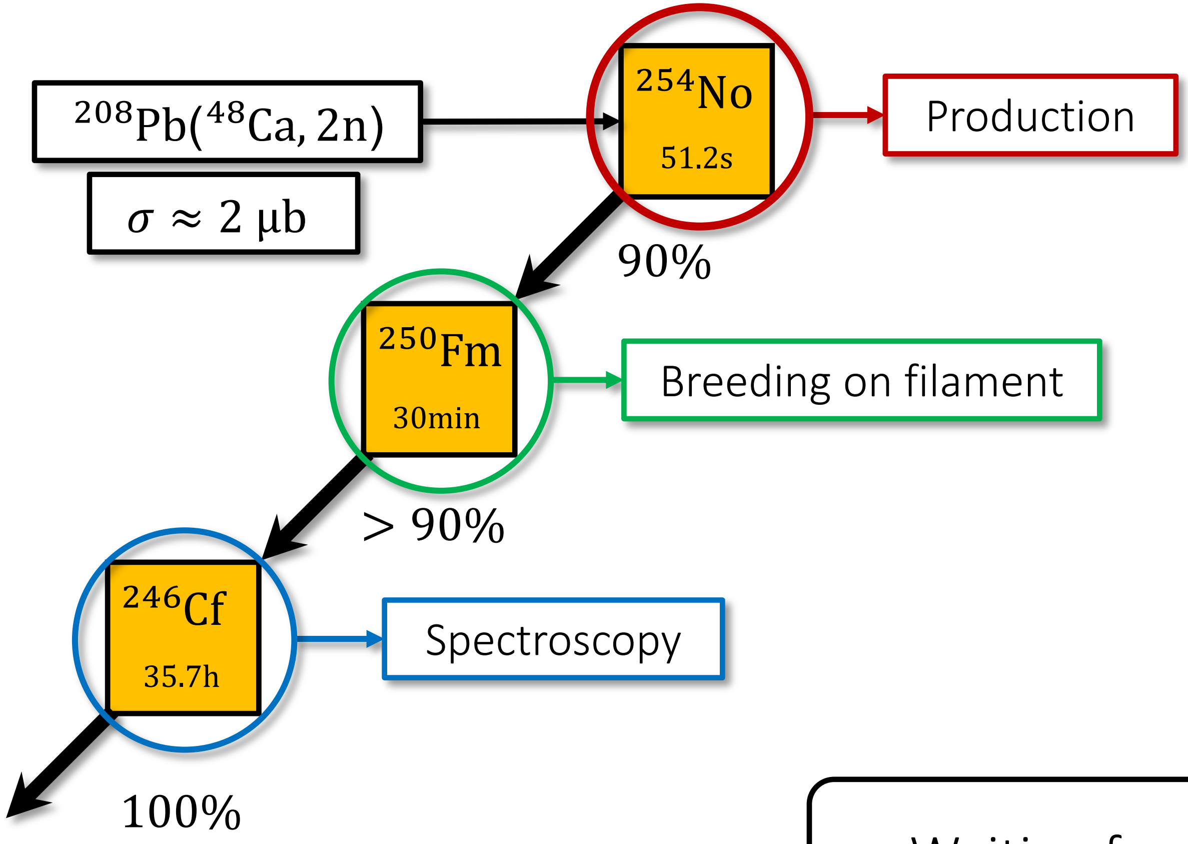

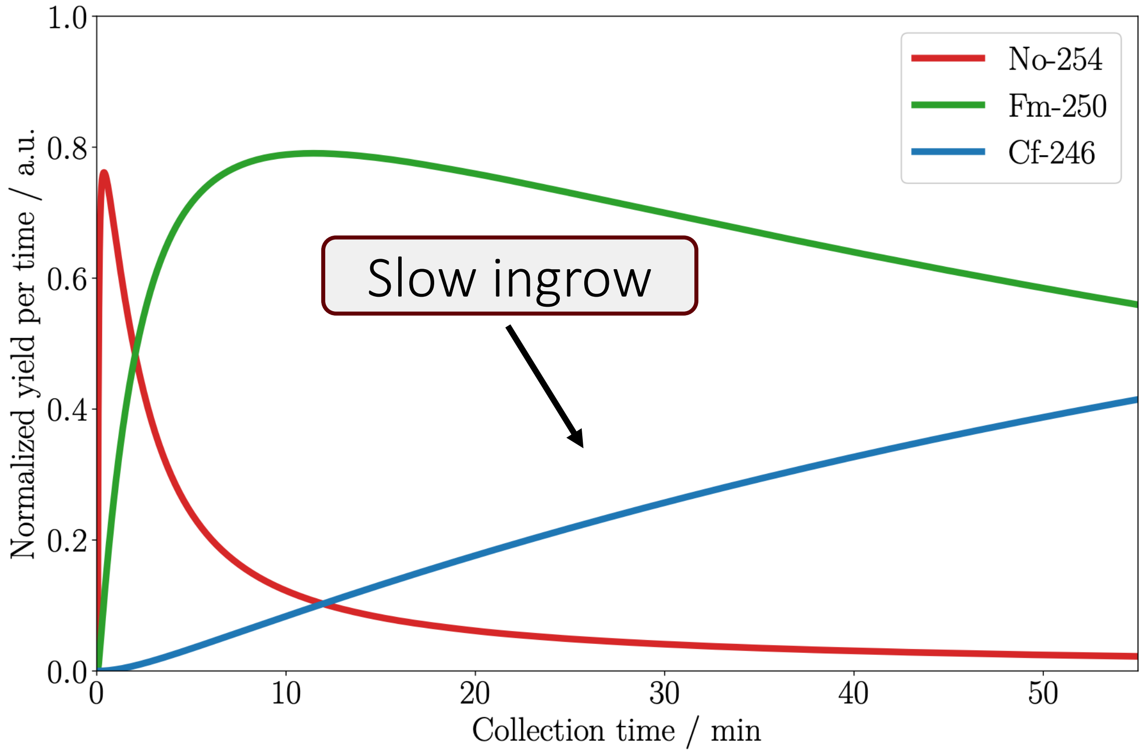

Waiting for maximized Cf yield unfeasible → compromise

TECHNISCHE UNIVERSITÄT DARMSTADT

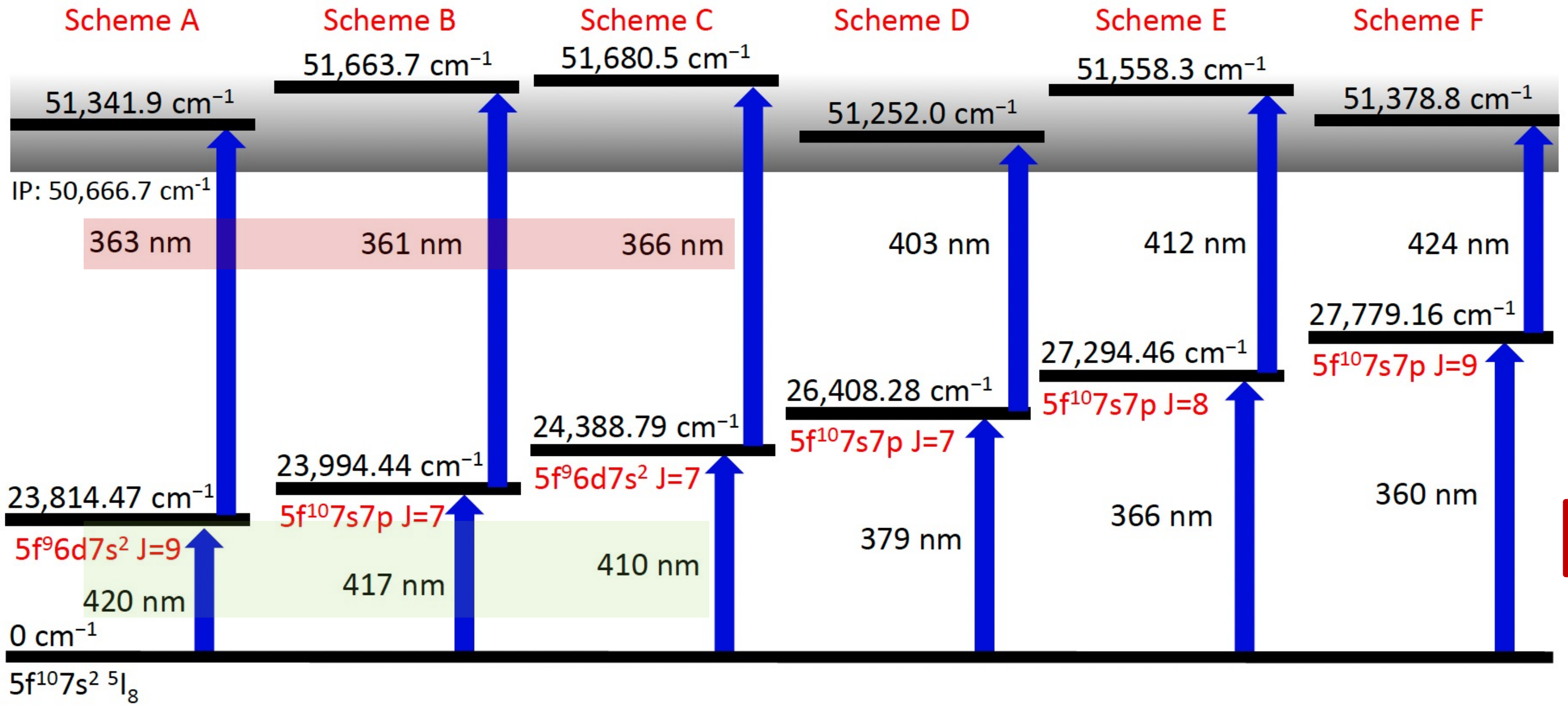

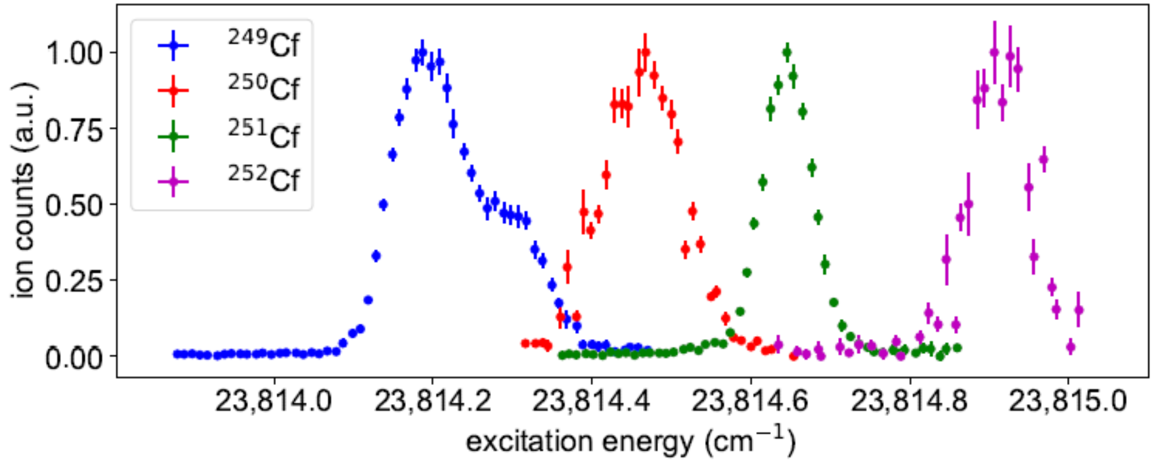

➤ Identified in ^{250}Cf

Non-Resonant

355 nm
28169.0 cm^{-1}

Resonant (AI)

DMQ	360	342-385

1st Step

Exalite 411	411	404 - 417
Exalite 417	419	413 - 422

Stilbene 3 aka Stilbene 420	425	419 - 434

TECHNISCHE UNIVERSITÄT DARMSTADT

Isotope	Reaction	α-Branch (%)	$\sigma_{\text{Production}}$ (nb)	$\sigma_{\text{Effective}}$ (nb)	$\sigma_{\text{Prod.}} / \sigma_{\text{Eff.}}$	Ions per hour
^{240}Cf	$^{195}\text{Pt}(^{48}\text{Ca}, 3\text{n})$	98	9	8.8	1.02	≈ 1
^{241}Cf	$^{196}\text{Pt}(^{48}\text{Ca}, 3\text{n})$	25	40	10	4	1 - 1.5
^{242}Cf	$^{196}\text{Pt}(^{48}\text{Ca}, 2\text{n})$	100	40	40	1	5 - 6
^{243}Cf	$^{198}\text{Pt}(^{48}\text{Ca}, 3\text{n})$	14	200	28	7.14	3.5 - 4
^{244}Cf	$^{198}\text{Pt}(^{48}\text{Ca}, 2\text{n})$	70(20)	100	70	1.42	9 - 10
^{245}Cf	$^{207}\text{Pb}(^{48}\text{Ca}, 2\text{n})$ 55% α, 15% α	35.3(25)	1000	29.12	34.4	0.3 – 0.4
^{246}Cf	$^{208}\text{Pb}(^{48}\text{Ca}, 2\text{n})$ 90% α, >90% α	100	1800	1458	1.23	18 - 22

$$\boxed{\sigma_{\text{Effective}} = \sigma_{\text{Production}} * \Pi_i \, \alpha_{\text{Branch},i}}$$

GSI